NUMERICAL SIMULATIONS OF MIXED-MODE DUCTILE FRACTURE INITIATION

R.Narasimhan
Department of Mechanical Engineering
Indian Institute of Science, Bangalore 560012

ABSTRACT

In this paper, an overview of computational studies on mixed-mode ductile fracture initiation (involving combination of modes I and II) is presented. These studies employ the Gurson constitutive model to represent the ductile fracture processes of micro-void nucleation, growth and coalescence and are carried out using a 2D plane strain boundary layer formulation. The specific issues that are addressed are the competition between micro-void coalescence and shear localization near a crack tip under mixed-mode loading and effects of void nucleation and (thickness) constraint on these processes. It is found that these two factors can profoundly influence the variation of ductile fracture toughness with mode mixity.

1. INTRODUCTION

In practical situations, the loading experienced at the tip of a crack could be very complex resulting in mixed-mode fracture. For ductile materials, the micro-structural processes that occur near a crack tip under mixed-mode (I and II) loading conditions, and which lead to ultimate material failure, involve a combination of micro-void coalescence and shear cracking [1,2]. However, some important issues pertaining to mixed mode ductile fracture are not fully understood. These involve a clear delineation of the competition between the above noted mechanisms, the role of specimen geometry and 3D effects near the crack tip. Further, contrasting trends have been reported in the literature on the variation of the fracture toughness for ductile materials with mode-mixity [2-4]. Thus, while experimental results given in [2,3] show a decrease in fracture toughness as the loading changes from mode I to II for a structural steel and aluminum alloy, respectively, another aluminum alloy studied in [4] shows the opposite behavior. The reasons for the different trends are not clear.

In this paper, some salient findings from computational studies on ductile crack initiation under combined mode (I and II) loading conditions [5-8] are presented with the view of resolving the above issues. These studies employ the Gurson constitutive model to represent the ductile fracture processes of micro-void nucleation, growth and coalescence. They are carried out using a plane strain boundary layer formulation, in which the mixed-mode elastic K-field and T-stress are prescribed as remote boundary conditions. The specific issues that are addressed are the competition between micro-void coalescence and shear localization near a crack tip under mixed-mode loading and effects of void nucleation and (thickness) constraint on these processes. It is found that these two factors can profoundly influence the variation of fracture toughness with mode mixity.

2. DUCTILE FRACTURE PROCESSES UNDER MIXED-MODE LOADING

In this section, some results which delineate the two ductile fracture processes of void coalescence and shear localization that are operative near a notch tip under mixed-mode loading are presented. These results are obtained from 2D plane strain finite element simulations of mixed-mode small scale yielding problem [5] corresponding to various values of remote elastic mixity parameter $\psi = \tan^{-1}(K_I / K_{II})$. The matrix material is assumed to exhibit power law hardening, with initial strain σ_o/E and hardening exponent chosen as 0.002 and 10. The void volume fraction at onset of coalescence and complete failure, f_c and f_F, are taken as 0.15 and 0.25, respectively.

The plastic zones for four cases of mode mixity are shown in Fig.1 using normalized Cartesian coordinates $x_1/(|K|/\sigma_o)^2$ and $x_2/(|K|/\sigma_o)^2$. The plastic zones are self-similar with respect to these axes. It can be seen from this figure that for mode I ($\psi = 90°$), the plastic zone spreads more above and below the notch tip. On the other hand, with increase in mode II component (decreasing ψ), the plastic zone extends further ahead of the crack tip (i.e., in the x_1 direction). Also, the maximum size of the plastic zone increases dramatically as ψ changes from 90° (mode I) to 0° (mode II).

The contours of normalized hydrostatic stress $\sigma_H/\sigma_o = \sigma_{kk}/(3\sigma_o)$ near the notch tip in deformed configuration are presented in Figs.2 (a) and (b) for $\psi = 90°$ and 30° at a value of $J/(\sigma_o b_o) = 3.4$ and 1.9, respectively. It is important to examine these contours because a large tensile hydrostatic stress promotes growth of micro-voids. First, it should be noted from these figures that the orientation of hydrostatic stress contours is rotated clockwise as ψ decreases from 90°. Secondly, the magnitude of the hydrostatic stress near the notch tip reduces as the mode II component increases. Thus, the peak value of σ_H/σ_o in Figs.2(a) and (b) is 3 and 1.7, respectively.

The contours of void volume fraction f and matrix plastic strain ε_m^p around the deformed notch for $\psi = 30°$ at $J/(\sigma_o b_o) = 3.45$ are shown in Figs.3(a) and (b). The length scale in these figures is set by the linear distance d between points P and Q which were located above and below the center of curvature of the notch in the undeformed configuration. The value of $d = 3.7b_o$ at the stage corresponding to Figs.3(a) and (b). It can be seen from Fig.3(a) that a part of the notch blunts while the remaining portion sharpens, and the maximum void volume fraction occurs near the blunted part. The level of f near the sharpened part (adjacent to point P) is small. This is due to the low level of hydrostatic stress in this region (see Fig.2(b)) and is in accord with experimental observations [2].

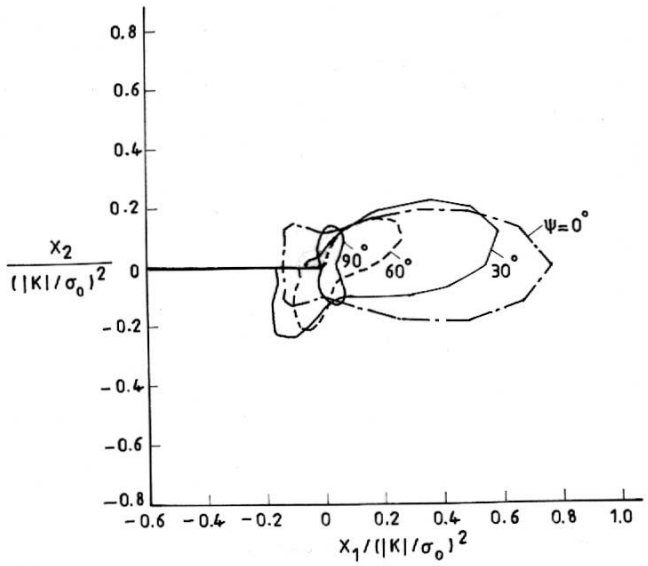

Fig.1 Plastic zones in normalized (self-similar) coordinates for various values of ψ.

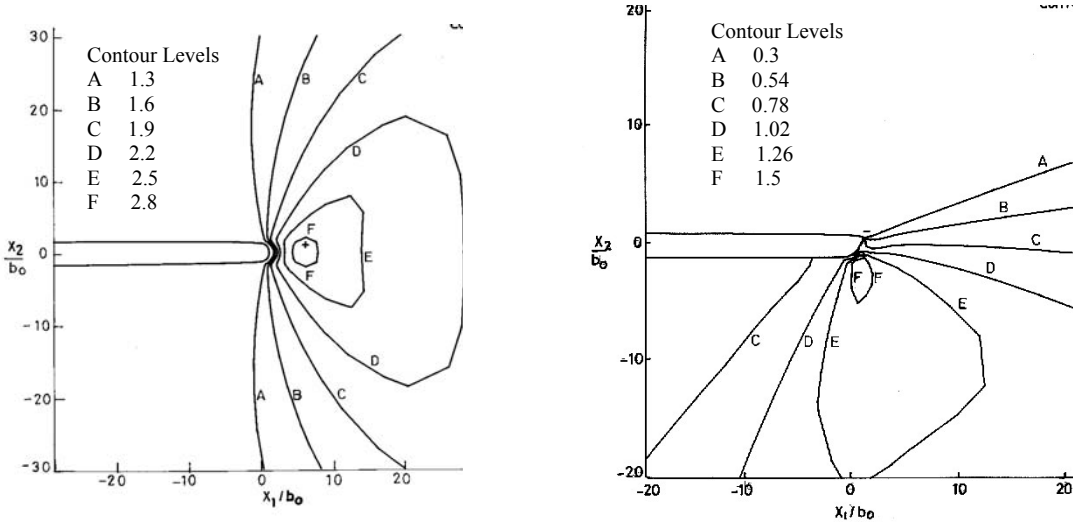

(a) (b)

Fig. 2 Contours of normalized hydrostatic stress σ_H/σ_o for (a) $\psi = 90°$ and (b) $\psi = 30°$.

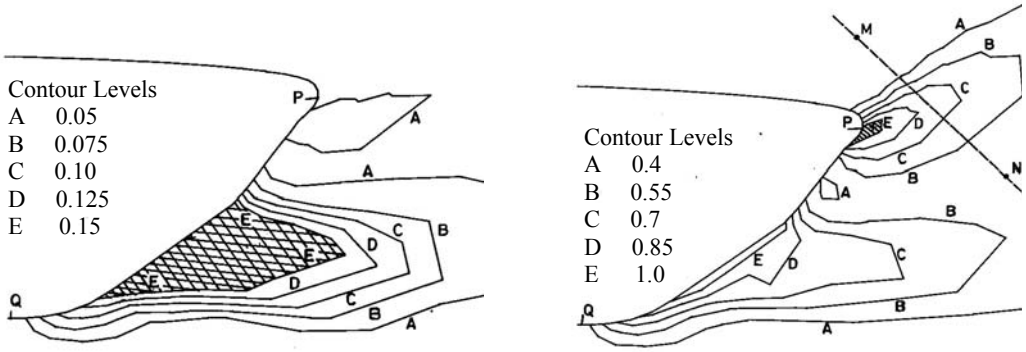

(a) (b)

Fig.3 Contours of (a) void volume fraction f and (b) matrix plastic strain ε_m^p near the notch tip for $\psi = 30°$ at $J/(\sigma_o b_o) = 3.45$.

The hatched region enclosed between the deformed notch surface and the innermost contour E in Fig.3(a) is the micro-void damage zone wherein, f has exceeded f_c and the material is close to failure. This zone strongly resembles the incipient fibrous crack from the blunted part of the notch observed by Tohgo et.al. [2] in their mixed-mode fracture experiments.

It can be noted from Fig.3(b) that large plastic strain has developed adjacent to both the sharpened as well as the blunted part of the notch. However, the contours near point P emanate in the form of a band from the sharpened portion of the notch which is due to intense shear deformation in this region. There is a large gradient of plastic strain within the band near point P which can be understood by examining the variation of ε_m^p along line MN that has been drawn across the band in Fig.3(b).

The material within this band can also experience failure by the propagation of a shear crack. If it is tentatively assumed that this would occur when ε_m^p within the band exceeds a critical value (of, say, 1.0), then the hatched zone in Fig.3(b) is likely to experience material failure. It is interesting to note that this strongly resembles the incipient shear crack observed in the experiments of Tohgo et.al. [2] for cases with a high mode II component.

3. VOID GROWTH NEAR A NOTCH TIP UNDER MIXED-MODE LOADING

In this section, the interaction between a pre-nucleated void and notch tip under mixed mode loading is examined. The results presented here are from boundary layer simulations undertaken in [6, 7], wherein the first and second terms of the elastic mixed-mode field involving K_I, K_{II} and T-stress were prescribed as remote boundary conditions. The details of the refined mesh near the notch tip used in these simulations is shown in Fig.4.

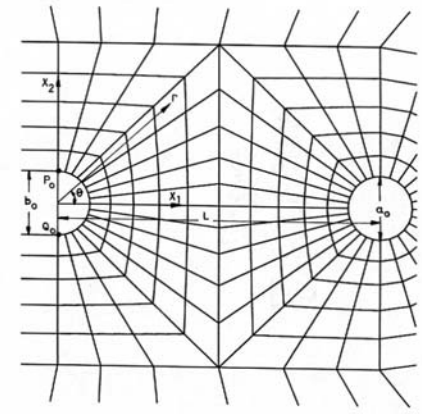

Fig.4 Finite element mesh showing notch tip and void ahead of it.

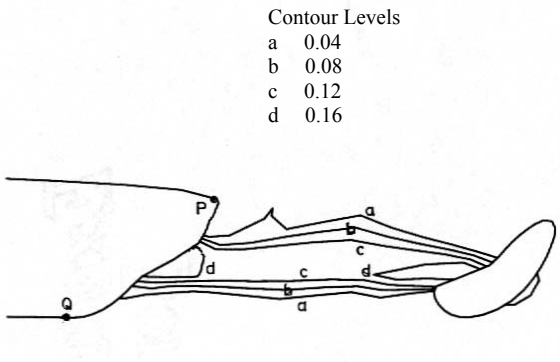

Fig.5 Contours of f near notch tip and void for $\psi = 30°$ and $T/\sigma_o = -0.75$.

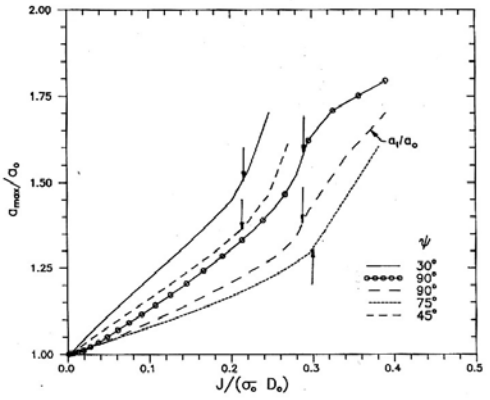

Fig.6 Variation of normalized maximum void diameter with $J/(\sigma_o L_o)$ for T=0.

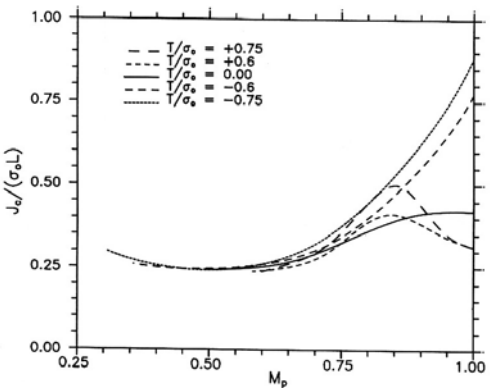

Fig.7 Variation of $J/(\sigma_o L_o)$ at fracture initiation with near-tip mixity for different T .

At a distance $L_o = 5b_o$ ahead of the notch tip, a circular void of radius $a_o = b_o$ is placed. The objective of using this model is to simulate the interaction between the notch tip and a nearby large void and the failure of the ligament connecting them by micro-void coalescence. In this context, fracture initiation is deemed to have taken place when this entire ligament experiences material failure. Thus, *the spacing between the notch tip and void is an important length scale of physical significance* in these simulations.

The contours of void volume fraction for $\psi = 30°$ and $T/\sigma_o = -0.75$ in a detailed region surrounding the deformed notch and void is shown in Fig.5. Due to large shear deformation in the ligament, the void has become skewed and elongated. Further, porosity has accumulated between the blunted part of the notch and void due to a good combination of plastic strain and hydrostatic tension. For mode II predominant loading as in Fig.5, it is found that the T-stress has little effect on the development of micro-void damage [7].

The normalized maximum void diameter a_{max}/a_o is plotted against $J/(\sigma_o L_o)$ for T=0 and different ψ in Fig.6. The stage at which incipient failure occurs in the ligament is indicated by a vertical arrow on curves shown in Fig. 6. It can be observed that a_{max}/a_o decreases initially as ψ is reduced from 90°, reaches a minimum at around $\psi = 75°$ and thereafter increases with further reduction in ψ. The former is due to drop in hydrostatic tension, whereas the latter is caused by increase in shear deformation in the ligament. The variations of normalized J at fracture initiation with near-tip plastic mixity defined as $M_p = 2/\pi(\tan^{-1}(\sigma_{\theta\theta}/\sigma_{r\theta}))$ immediately ahead of the tip for different T are shown in Fig.7. It may be seen that for negative T, the critical value of J reduces with decrease in M_p owing to increased shear deformation in the ligament, whereas for positive T, there is an initial increase followed by a strong reduction. T-stress has negligible influence on J_c for M_p less than 0.5.

4. EFFECT OF VOID NUCLEATION ON MIXED-MODE FRACTURE

In this section, a few results from a numerical simulation [8] depicting mixed-mode fracture in an alloy with a dual population of void nucleating particles are presented. Void nucleation at small, uniformly distributed particles is assumed to be strain-controlled, whereas an interface stress-controlled mechanism is employed to simulate porosity development at large inclusions which are arranged in a rectangular array (see [8] for details). A distribution of large *synthetic inclusions* surrounding the notch tip is illustrated in Fig.8. The contours of f for $\psi = 30°$ are shown in Fig.9.

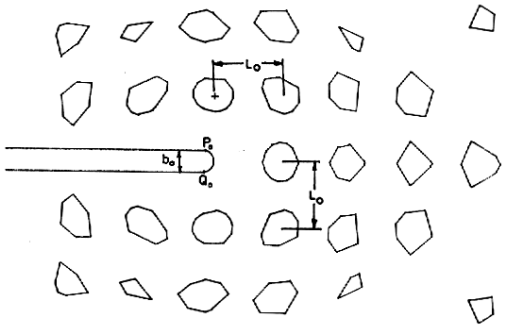

Fig.8 Distribution of *synthetic inclusions* around notch tip ($L_o/b_o = 3$).

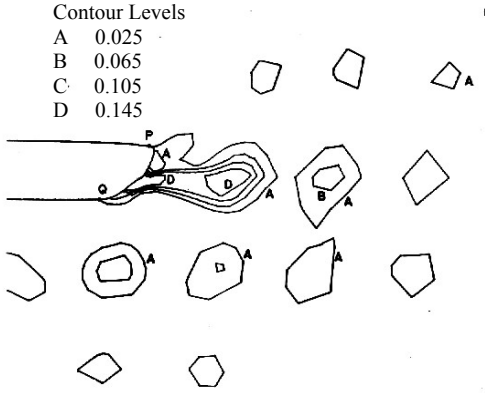

Fig.9 Contours of void volume fraction for $\psi = 30°$.

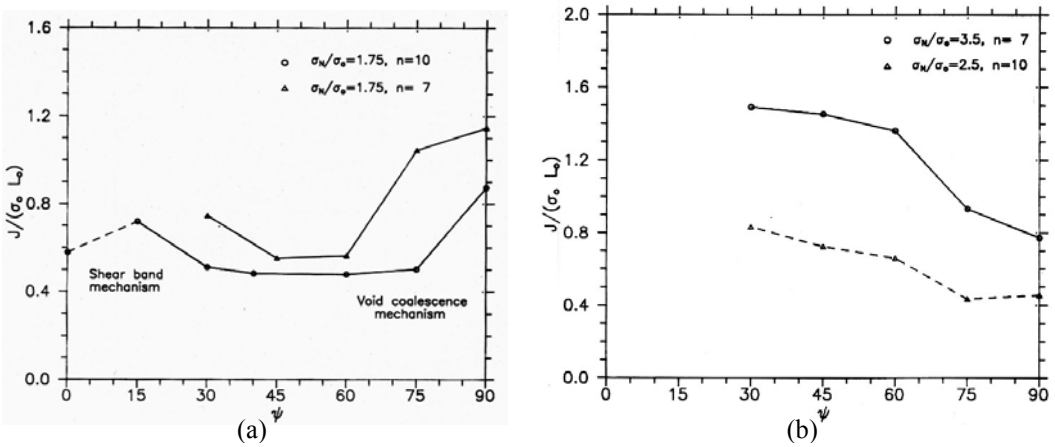

Fig.10 Variation of $J/(\sigma_o L_o)$ at fracture initiation with ψ for (a) low and (b) high void nucleation stress.

It can be observed from Fig.9 that porosity has developed around the synthetic inclusions over a wide region surrounding the notch tip especially in the lower-half region adjacent to the blunted part of the notch. Also the entire ligament connecting this part of the notch with the first inclusion site has failed by micro-void coalescence which is similar to Fig.5. In Figs.10(a) and (b), the predicted fracture toughness is plotted against ψ for low and high void nucleation stress σ_N, respectively. Fig.10(a) shows that J_c due to micro-void coalescence mechanism decreases with ψ from 90°, reaches a minimum between 45° and 30°, and thereafter increases (which is similar to Fig.7). Further, for ψ less than 15°, failure by shear localization from the sharpened part of the notch is the preponderant failure mechanism which corroborates with experimental results [2]. Also, higher strain hardening (smaller n) retards failure by micro-void coalescence irrespective of ψ. In contrast to Fig.10(a), it can be seen from Fig.10(b) that for high σ_N , J_c increases with mode II component owing to the delay in void nucleation around the synthetic inclusions [8].

5. CONCLUDING REMARKS

The simulations presented in this paper have clearly delineated the competition between void coalescence and shear localization near a crack tip under mixed-mode loading. Also, they have demonstrated that crack tip constraint and void nucleation stress can profoundly influence the variation of fracture toughness with mode-mixity for ductile materials.

REFERENCES

1. Otsuka, A., Tohgo, K., Okamato, Y., Relationship between ductile crack initiation and void volume fraction, *Nucl. Engng. Des.,* 105, 121-129, 1987.
2. Tohgo, K., Otsuka, A., Gao H.W., The behavior of ductile crack initiation from a notch under mixed-mode loading, *Proc.Far East Fracture Group Workshop*, Tokyo Inst. Tech., pp.101-108, 1988.
3. Kamat, S.V., Hirth, J.P., *Acta mater*., 44, p.201, 1996.
4. Aoki, S., Kishimoto, K., Yoshida, T., Sakata, M., Richard, H.A., Elastic-plastic fracture behavior of an aluminum alloy under mixed-mode loading, *J.Mech.Phys. Solids*, 38, 195-213, 1990.
5. Ghosal, A.K., Narasimhan, R., A finite element analysis of mixed-mode fracture initiation by ductile failure mechanisms*, J.Mech.,Phys. Solids*, 42, 953-978, 1994.
6. Ghosal, A.K., Narasimhan, R., Numerical simulations of hole growth and ductile fracture initiation under mixed-mode loading, *Int.J.Fract*ure, 77, 281-304, 1996.
7. Arun Roy, Y., Narasimhan R., Constraint effects on ductile fracture processes near a notch tip under mixed-mode loading, *Engng.Fract. Mech*., 62, 511-534, 1999.
8. Ghosal, A.K, Narasimhan, R., Mixed-mode fracture initiation in a ductile material with a dual population of void nucleating particles, *Mater Sci. Engng*. A, 211, 117-127, 1996.